Environment International 199 (2025) 109473

Contents lists available at ScienceDirect

Environment International

journal homepage: www.elsevier.com/locate/envint

Full length article

Dynamic biodistribution of inhaled silica particles to extrapulmonary sites: Early and late translocation mechanisms with implication for particle biomonitoring

Riccardo Leinardi [a,*], Chiara Longo Sanchez-Calero [a], Saloua Ibouraadaten [a], Francine Uwambayinema [a], Yousof Yakoub [a], Cristina Pavan [b,c], Rani Claus [d,e], Frauke Lemaire [d,e], Steven Ronsmans [d], Manosij Ghosh [d,e], Lénárd Farczádi [f], Horatiu Moldovan [g], Jeroen A.J. Vanoirbeek [d,e], Francesco Turci [b,c], Peter H.M. Hoet [d,e], François Huaux [a]

[a] Louvain Centre for Toxicology and Applied Pharmacology (LTAP), Institute of Experimental and Clinical Research (IREC), Université Catholique de Louvain (UCLouvain), Avenue Hippocrate 57, 1200 Woluwe-Saint-Lambert, Brussels, Belgium
[b] Department of Chemistry, University of Turin, Via P. Giuria 7, 10125 Turin, Italy
[c] "G. Scansetti" Interdepartmental Centre for Studies on Asbestos and Other Toxic Particulates, University of Turin, Via P. Giuria 7, 10125 Turin, Italy
[d] Environment and Health Unit, KU Leuven, Herestraat 49, 3000 Leuven, Belgium
[e] Laboratory of Respiratory Diseases and Thoracic Surgery (BREATHE), KU Leuven, Herestraat 49, 3000 Leuven, Belgium
[f] Center for Advanced Medical and Pharmaceutical Research, George Emil Palade University of Medicine, Pharmacy, Science, and Technology (UMFST), Gh. Marinescu 38, 540142 Târgu Mureş, Romania
[g] Department of Occupational Medicine, Faculty of Medicine, George Emil Palade University of Medicine, Pharmacy, Science and Technology (UMFST), Gh. Marinescu 38, 540142 Târgu Mureş, Romania

ARTICLE INFO

Keywords:
Crystalline silica
Biodistribution
Particle translocation
Silicon
Exposure
Biomonitoring
Biomarker

ABSTRACT

An innovative method based on inductively coupled plasma mass spectrometry (ICP-MS) was developed to quantify the time-dependent systemic redistribution pattern of pulmonary-deposited crystalline silica particles by measuring silicon (Si) levels in the lungs, distal organs, and biological fluids. The method was applied in a murine model and validated in blood and urine samples from two occupationally exposed cohorts (miners and porcelain industry workers). In mice, 30 % of silica particles deposited in the lungs via oropharyngeal administration accumulated in extrapulmonary sites in less than 4 months. An early translocation (within 3 days) resulted in silica distribution to liver and kidneys (13 %), followed by a delayed migration (up to 60 days) in mediastinal lymph nodes (12 %), spleen (1.7 %), and abdominal skin (1.7 %). The long-term increase of Si in urine suggested silica renal clearance. Our data also indicated that the toxic potential of particles is a key determinant of extrapulmonary redistribution. The interest of Si as biomarker of exposure has been confirmed in workers exposed to crystalline silica dust. In these individuals, elevated Si levels in blood and urine paralleled silica exposure. Our findings quantify the dynamics of silica biodistribution in extrapulmonary organs, offering new insights on the biomonitoring of silica exposure in different scenarios.

1. Introduction

Inhalation of crystalline silica (CS, crystalline silicon dioxide, SiO_2) dusts in respirable size (respirable crystalline silica – RCS) is associated with an increased risk of developing severe pulmonary diseases including silicosis, bronchitis, obstructive pulmonary disease and lung cancer (IARC, 2012; Sato et al., 2018; Hoy and Chambers, 2020). A particular subfamily of surface moieties, namely the nearly free silanols (NFS), was identified as the molecular initiator of crystalline (and amorphous) silica toxicity. NFS are a specific family of silanol (Si-OH) groups appearing on crystalline silica particles upon mechanical fracturing and reaction with environmental water vapor (Pavan et al.,

* Corresponding author.
E-mail address: riccardo.leinardi@uclouvain.be (R. Leinardi).

https://doi.org/10.1016/j.envint.2025.109473
Received 11 October 2024; Received in revised form 11 April 2025; Accepted 14 April 2025
Available online 15 April 2025

2020). Their key role in activating alveolar macrophages and triggering short- and long-term pulmonary responses to silica has been recently described in in vitro and in vivo investigations (Pavan et al., 2020; Leinardi et al., 2023; Pavan et al., 2023; Pavan et al., 2024). Apart from local effects, a range of non-respiratory conditions is associated with crystalline silica exposure, including renal alterations, liver granulomas (Osorio et al., 1987; Mohner et al., 2017; Guarnieri et al., 2019; Marinaccio et al., 2006; Ibrahim et al., 2011; Vupputuri et al., 2012) and autoimmune disorders (Rubio-Rivas et al., 2017; Parks et al., 2002; Ferri et al., 2018; Aguila et al., 2021; Boudigaard et al., 2021; Morotti et al., 2022; De Decker et al., 2018). These detrimental responses might be associated with the migration of inhaled particles to specific extrapulmonary target sites (Parks et al., 1999). Indeed, multiorgan silicosis and particle accumulation in liver, kidneys and peripheral immune organs in exposed workers strongly suggest particle systemic distribution (Guarnieri et al., 2019; Ibrahim et al., 2011; Giles et al., 1978).

Inhaled crystalline silica particles are believed to be cleared from the lungs through several routes, including (i) muco-ciliary transport in the bronchial and tracheal regions leading to their transfer to the gastrointestinal tract, (ii) migration to the thoracic lymph nodes, and (iii) absorption into the bloodstream and/or lymphatic system, followed by transport to other body compartments (Nakane, 2012; Stuart, 1984; Wang et al., 2022; Kuempel et al., 2015). A possible role in the extrapulmonary distribution of particles deposited in the lungs, including silica, has been recently attributed to interstitial and/or alveolar lung megakaryocytes activated during inflammatory responses (Qiu et al., 2024). However, the exact mechanisms and the rate of crystalline silica undergoing systemic translocation and extrapulmonary deposition remain poorly understood. In addition, the association between crystalline silica exposure and extrapulmonary diseases is still poorly investigated and represents a crucial research area with potential implications for occupational health and public policy, particularly concerning silica exposure limits and protective measures across various industrial contexts. The difficulty in establishing a direct biomarker of exposure makes RCS biomonitoring extremely challenging. In a previous report, the quantification of silica by measuring silicon (Si) in exhaled breath condensates of RCS-exposed workers was proposed (Leese et al., 2017). However, this approach entails several limitations, chiefly stemming from the limited sample volume of sample obtained.

The translocation of crystalline silica particles from the respiratory system to peripheral organs remains therefore an area of ongoing research and debate (Hoy and Chambers, 2020). Furthermore, a biokinetic model detailing the degree of systemic translocation of crystalline silica following pulmonary deposition, is still missing. Choosing the correct analytical approach to monitor particle biodistribution in the body is also crucial, considering the low concentrations of particles accumulated in the organs, and the extreme complexity of biological tissues (Wang et al., 2022; Leese et al., 2017). Because of the abundance of silica in the environment, the development of a reliable protocol to biomonitoring crystalline silica exposure is extremely challenging (Leese et al., 2017). Classical dissolution protocols involve hydrofluoric acid (HF) to solubilize SiO_2 and make Si ions available for quantification via the generation of soluble Si-F complexes. However, the use of HF has several technical drawbacks, including high toxicity and instrumental damage (Kirkpatrick et al., 1995; Wang et al., 2014). To overcome these barriers, we developed a novel ICP-MS approach based on a non-acidic digestion by treating the biological mixture with concentrated NaOH, which is known to efficiently solubilize crystalline silica (Cai et al., 2008; Bossert et al., 2019). This alkaline digestion converts particle Si into its ionic form, which can therefore be measured in a safer way with respect to HF-based approaches.

In the present study, we applied the alkaline digestion of tissue and ICP-MS analysis to monitor the time-dependent biodistribution of crystalline silica particles following pulmonary administration in a mouse model. The methodology was validated with urine and blood samples from coal mine and porcelain industry workers. A group of office workers without occupational silica exposure was recruited as control.

2. Materials and methods

2.1. Crystalline silica particles

Synthetic as-grown crystalline silica particles (gQ) were prepared and characterized in the laboratories of centre "G. Scansetti" (University of Turin, Italy) following an established procedure, with minor modifications (Pavan et al., 2020; Pastero et al., 2016). Briefly, a 25 % (w/w) sodium-metasilicate pentahydrate (NAMTS) aqueous solution was polymerized using mineral acids until gel formation (pH ca. 8). Growth runs (168 h) in PTFE liner sealed into steel autoclaves were performed at 210 °C and autogenic pressure. Crystallinity was verified by X-ray diffraction (XRD). One gram of synthetic crystalline silica was sieved in a double sieve with 100- and 30-μm meshes on a vibrating apparatus for 30 min. The fraction with size < 30 μm was used as such (gQ), while the fraction > 30 μm (500 mg) was ground in an MM200 mixer mill (Retsch, Düsseldorf, Germany) in agate jars (2 spheres, 6 mm, 27 Hz, 6 h) to obtain gQ-f crystals (micrometric and synthetic fractured crystalline silica). nQ-f (nanometric and synthetic fractured crystalline silica) was prepared following a procedure reported by Bellomo (Bellomo et al., 2022). A 1.5 g of gQ was milled with a planetary mill (Pulveirisette 6, Fritsch, Idar-Oberstein, Germany) in a ZrO_2 jar using ZrO_2 spheres (total mass = 41 g, diameter = 5 mm) at 450 rpm for 1 h, with a pause of 1 min every 20 min. This finely milled precursor (1.5 g) was then further milled in the same apparatus, by adding 12 ml of ultrapure water previously filtered through a 0.22 μm filter, and using ZrO_2 spheres (diameter = 2 mm, total mass = 41 g). Wet milling was carried out for 2 h at 550 rpm. After milling, the obtained dust was sedimented for 24 h. The supernatant was recovered and dried in an oven at 60 °C to obtain nQ-f particles.

Min-U-Sil 5 (U.S. Silica Co., Berkeley Springs, WV, USA; lot number 15062696) is a commercial fractured microcrystalline α-quartz largely used in studies of experimental silicosis and/or lung cancer (IARC, IARC Working Group on the Evaluation of Carcinogenic Risks to Humans: Silica, Some Silicates, Coal Dust and Para-Aramid Fibrils. Lyon, 15-22 October, 1996). All the samples were deeply characterized in previous studies (Pavan et al., 2020; Leinardi et al., 2023; Bellomo et al., 2022; Pavan et al., 2022). Their main physico-chemical properties are summarized in Table 1.

2.2. Particle preparation for animal studies

The particles were heated at 200 °C for 2 h just prior to suspension to inactivate any trace endotoxin. Stock suspensions prepared in 0.9 % NaCl were ultrasonicated on ice (3 min, 100 W, probe diameter 3 mm) using a VCX 750 ultrasonic processor (Sonics, Newtown, CT, USA), and then sonicated in a bath for 15 min to ensure dissociation of particle agglomerates (total delivered energy 27 kJ).

2.3. Animals

Twelwe-week-old female C57BL/6 mice (weight: 20 g) were purchased from Janvier SAS (St Berthevin, France). The mice were housed in polycarbonate cages with conventional sawdust (Carfil, Oud-Turnhout, Belgium) in a controlled environment (25 °C, 50 % relative humidity) with acidified water and food ad libitum. To limit silicon (Si) background in the tissues, a standard rodent diet low in Si was selected. All experimental processes were in accordance with the NIH Guide for the Care and Use of Laboratory animals, and Belgian and European regulations (EEC n ° 86/609, LA1230312 and 2022/UCL/MD/019).

2.4. Particle exposure and tissue collection for ICP-MS analysis

The mice (n = 144) were divided into five main groups: unexposed to

Table 1
Physico-chemical properties of the crystalline silica samples used in the present study.

Sample	Origin (Type)	Surface state	Particle size (μm ± SD)[a]	SSA (m^2/g)[b]	NFS content[c]	Ref.
Min-U-Sil 5	Commercial (α-quartz)	Fractured	1.3 ± 0.6	4.3	high	(Pavan et al., 2024; Leinardi et al., 2020)
nQ-f	Synthetic (α-quartz)	Fractured	0.28 ± 0.016*	55	high	(Bellomo et al., 2022)
gQ	Synthetic (α-quartz)	As-grown	1.3 ± 2.3	5.8	no/low	(Pavan et al., 2020; Leinardi et al., 2020)
gQ-f	Synthetic (α-quartz)	Fractured	1.2 ± 0.7	4.5	high	(Pavan et al., 2020; Leinardi et al., 2020)

[a] Measured by flow particle image analysis (FPIA) in ultrapure H_2O;
[*] Measured by dynamic light scattering (DLS) analysis in ultrapure H_2O;
[b] Specific surface area (SSA) measured by the Brunauer-Emmett-Teller (BET) method using Kr or N_2 depending on the expected SSA value;
[c] Nearly free silanols (NFS) assessed by FT-IR spectroscopy.

silica (Ctrl, n = 48), Exposed A (Min-U-Sil, n = 48), Exposed B (nQ-f, n = 16), Exposed C (gQ, n = 16), Exposed D (gQ-f, n = 16). Each group was further divided into different sub-groups, in accordance with the time interval investigated: 15 min, 3 h, 1 day, 3 days, 60 days, and 120 days post particle exposure. Ctrl and Exposed A (Min-U-Sil) mice were divided into six sub-groups (n = 8/group) per each of the time intervals investigated. Exposed B (nQ-f), C (gQ) and D (gQ-f) were divided into two subgroups: Exposed B, 15 min (n = 8) and 3 d (n = 8), Exposed C and D, 15 min (n = 8) and 120 d (n = 8). Silica-exposed mice received 50 μl of particle suspension (2.5 mg/mouse, single exposure) directly into the lungs via oropharyngeal aspiration (o.p.a). The dose of 2.5 mg silica/mouse was previously described in the literature as effectively inducing acute and chronic pulmonary responses for NFS-rich quartz particles (Huaux et al., 2002; Giordano et al., 2010). Control mice received 50 μL of 0.9 % NaCl. All administrations were performed on anesthetized mice with a mix of 1 mg Ketalar (N.V. Warner-Lambert, Zaventem, Belgium) and 0.2 mg Rompun (Bayer A6, Leverkusen, Germany). Animals were sacrificed via an intraperitoneal injection of 60 mg/ml (200 μl, intraperitoneal) sodium pentobarbital (Certa, Braine-l'Alleud, Belgium). After being sacrificed, the lungs, liver, kidneys, mediastinal lymph nodes, spleen, and abdominal skin specimens (ca. 1 cm diameter) of control and silica-exposed mice were surgically removed, washed with saline to avoid potential contamination, and homogenized with an Ultra-Turrax T25 homogenizer (Janke and Kunkel, Brussels, Belgium) for further analysis. Blood was collected via cardiac puncture (ca. 1.2 ml/mouse) in Eppendorf microcentrifuge tube with anticoagulant (EDTA). 700 μl of blood were later transferred in a clean tube and centrifuged for 15 min (1,500 x g) at 4 °C. The supernatant (plasma) was then further transferred to a 0.5 ml-Eppendorf tube. Urine samples (< 1 ml) were collected before the sacrifice by applying gentle pressure to the caudal area of the back of the mouse. The samples were stored at −80 °C until ICP-MS analysis.

2.5. Particle exposure and tissue collection for histology and imaging

An additional set of mice unexposed (Ctrl, n = 6) or exposed 120 days to Min-U-Sil 5 crystalline silica (n = 6; 2.5 mg/mouse, 50 μl) was dedicated to histology and imaging. Control animals were treated with saline (50 μl). Mice were sacrificed as explained above. Selected organs (lung, liver, kidney, lymph nodes, and spleen) collected from these animals were excised, washed with saline and recovered in 3.65 % paraformaldehyde (Sigma-Aldrich, St. Louis, MO, USA) in PBS for histological analysis. After overnight fixation, the whole organ was embedded in paraffin blocks. Serial sections of 5 μm thickness were cut and stained with hematoxylin and eosin (H&E, nucleus and cytoplasm staining). Images were collected in brightfield and polarized light using an Axioscan.Z1 slide scanner (ZEISS, Oberkochen, Germany), and processed with ZEISS ZEN 3.8 image analysis software.

2.6. Population study

Male subjects working at the same coal mine were included (Mine Workers, n = 75; median age = 40, smokers and non-smokers, exposed to crystalline silica dusts from 1 to 22 years). Porcelain industry workers (n = 60; median age = 45, smokers and non-smokers, exposed from 2 to 45 years to industrial dust containing crystalline silica) from the same production facility were included in the study as an additional occupationally exposed group. The unexposed group is a control group (Ctrl, n = 61; median age = 45, smokers and non-smokers, office workers without occupational silica exposure). All study subjects were interviewed using a structured questionnaire developed ad hoc. The study was approved by the Ethics Committee of the University of Medicine and Pharmacy of Tîrgu Mureş, Romania (regulation code UMFST-REG-74-F01-Ed.02, registration number 5038, registration date August 20th, 2021). A collaboration protocol was established with the factory where the workers are performing. Due to the confidentiality provisions, factory's name and location, except the country (Romania), cannot be disclosed. Subjects included in the study received information about the objectives of the project, and signed an informed consent issued in accordance with the Helsinki declaration. Demographic of the workers (age, gender, seniority at work) and laboratory data, as well as biological samples were used only for the purpose of the study protocol. No names were used, and the subject's privacy/anonymity were preserved. Volunteers' characteristics are summarized in the Supplementary materials (Table S1).

2.7. Sample collection

Whole blood (6 ml, Ctrl and Mine Workers) was obtained by venipuncture, and collected in Vacutainer K2EDTA tubes (BD, Franklin Lakes, NJ, USA). 2 ml were stored at – 80 °C. The remaining part (4 ml) was transferred to a clean Vacutainer tube and centrifuged at 2,000 g for 10 min at room temperature within 2 h by collection to separate plasma. Plasma samples (Ctrl and Mine Workers) were then transferred in clean cryovials tubes and stored at – 20 °C. Urine samples (Ctrl, Mine Workers, and Porcelain Workers) were collected in carbon-free HDPE jars (LP Italiana Spa, Milan, Italy). After the collection, the samples were shipped to Belgium and stored at – 80 °C prior to analysis. In total, the following human samples were analyzed:

- Blood samples: Ctrl, n = 61; Mine Workers, n = 75;
- Plasma samples: Ctrl, n = 34; Mine Workers, n = 41;
- Urine samples: Ctrl, n = 61; Mine Workers, n = 75; Porcelain Workers, n = 60.

2.8. Quantitative analysis of silicon levels in organs and fluids collected from animals and humans via ICP-MS

Crystalline silica exposure was biomonitored in murine organs (lung, liver, kidneys, mediastinal lymph nodes, spleen, and skin), and urine, whole blood and plasma obtained from mice or humans. To this, silicon (Si) levels were quantified via inductively coupled argon/helium plasma mass spectrometry (ICP-MS), using an Agilent 7500ce Octopole Reaction System (Agilent Technologies, Santa Clara, USA). The approach (summarized in Fig. 1) was developed in accordance with the study from Hoet (Hoet et al., 2013). Prior to ICP-MS measurement, 500 µl of tissue homogenates or urine/blood/plasma collected from control and exposed mice or control and exposed humans were transferred into PTFE reactors and mineralized at 200 °C for 2 h in alkaline environment (approx. pH 15) obtained via the addiction of two NaOH pellets (200 mg). The residue was dissolved by adding 4600 µl of ultrapure H_2O and neutralized with 400 µl concentrated HNO_3 (14 M). Then, 500 µl of the mixture were transferred into disposable polypropylene tubes and diluted quantitatively (1 + 9) in ICP-MS diluent (a 0.5 % HCl, 1 % HNO_3 solution containing Sc, Ir, Ge, Rh as internal standards). The resulting mixture was then injected into the spectrometer for the determination of Si content. The use of glass equipment was avoided during sample preparation to prevent Si contamination. All sample manipulations were carried out in clean room conditions, under laminar flow. TraceCERT silicon standard (Sigma-Aldrich, St Louis, MO, USA; 10,000 mg/l Si in nitric acid) was used for Si quantification. Laboratory duplicates were included in all analyses. The carry-over effect from previous measurements was reduced performing rinsing between the samples with 2 % HNO_3 for 60 s, followed by rinsing with 1 % HNO_3 for 30 s. Limits of detection (LoD, 3.51 µg/l) and quantification (LoQ, 10.54 µg/l) were calculated as the standard deviation of the blank (three and nine times, respectively) (Hoet et al., 2021). The instrument set-up is summarized in the Supplementary materials (Table S2).

3. Results

3.1. An early and progressive reduction of pulmonary silica burden follows particle administration in the lungs

To biomonitor the persistence of silica particles in the lungs, we first quantified crystalline silica pulmonary burden 15 min (15 min), 3 h (3 h), 1 day (1 d), 3 days (3 d), 60 days (60 d) and 120 days (120 d) after administration in animals (Fig. 2A). Mice were treated with crystalline silica (Min-U-Sil 5, 2.5 mg/mouse) via oropharyngeal aspiration (o.p.a.). The mass (mg) of particles accumulated in the lungs was quantified by measuring the level of silicon (Si) in mineralized lung homogenates via ICP-MS. The dose measured in the lungs fifteen minutes after administration (baseline value), corresponding to 1.25 mg of SiO_2 (i.e., 50 % or the instilled dose), was considered as the effective deposited particle dose (Fig. 2B). We then quantified silica burden at specific time intervals representative of acute- and long-term responses to crystalline silica (Giordano et al., 2010; Rabolli et al., 2014; Huang et al., 2019). A sustained time-dependent decrease in pulmonary silica content was observed. Indeed, 34 % (0.45 mg) of silica initially deposited in the lungs was removed during the first 3 days following the exposure. At 60 days, around 45 % (0.58 mg) of silica was cleared from the lungs. Between day 60 and 120, a plateau in the residual particle burden was reached, and no further clearance was observed (Fig. 2B). We concluded that pulmonary-deposited crystalline silica was rapidly, and progressively, transported out of the lungs.

Physico-chemical properties affect the pulmonary retention of particles deposited in the lungs (Nemmar et al., 2001; Choi et al., 2010; Liu et al., 2020). Therefore, we first hypothesized that particle size may play a relevant role in driving translocation. This was evaluated by treating mice with membranolytic synthetic crystalline silica particles (nQ-f) in nanometric size with an average hydrodynamic diameter of ca. 300 nm (see Table 1) (Bellomo et al., 2022). Early translocation of nQ-f was compared with Min-U-Sil 5 silica particles, characterized by diameters in the micrometric range (1.3 ± 0.6 µm). In line with Min-U-Sil 5, a substantial decrease (approx. 50 % of the deposited silica dose) was noticed at 3 d in nQ-f burden (Fig. 2C). This result suggested that particle size was not a primary factor in determining crystalline silica translocation.

We then evaluated whether particle toxicity was implicated in the translocation process. To this, we used two synthetic quartz samples showing comparable size but contrasting toxic potential due to different nearly free silanols (NFS) content (gQ-f: NFS-rich, toxic; gQ: NFS-poor, low toxic). This specific subgroup of surface silanols (Si-OH) was recently pointed out as the primary determinant of silica pathologic activity, because of the ability to interact with cell membrane epitopes, leading to membrane disruption (Pavan et al., 2020; Pavan et al., 2022). After exposing mice to NFS-rich gQ-f or NFS-poor gQ, we found that the toxicity effect determined by the NFS content played a critical role in the translocation process. Data suggested that gQ particles with low toxicity were retained in the lungs to a significantly greater extent when compared to the more toxic gQ-f. Indeed, 25 % of the gQ-f particles deposited in the lungs were cleared 120 days post treatment when compared to 15 min, whereas no time-dependent change in particle load was observed in the lungs of mice exposed to gQ (Fig. 2D).

Overall, these results indicate that crystalline silica deposited in the lungs was rapidly and continuously cleared until reaching a plateau, in a process driven by particle toxic potential rather than size.

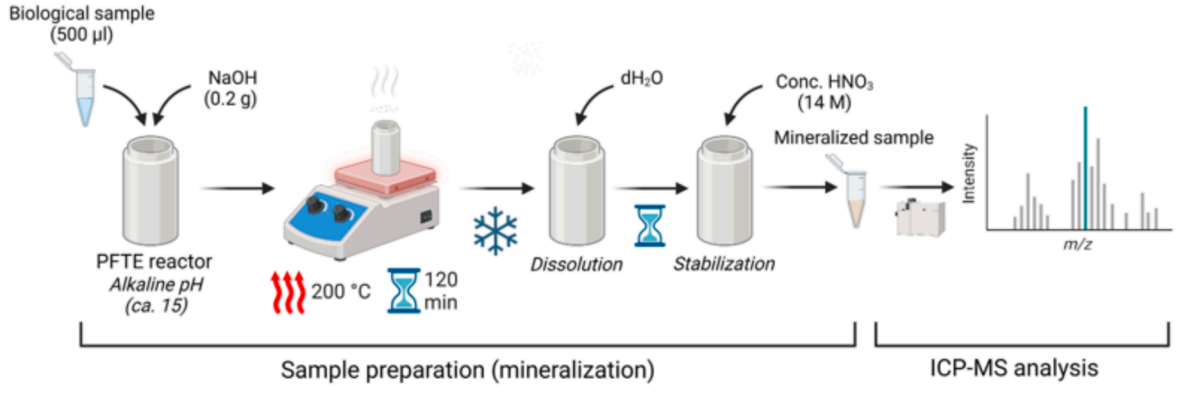

Fig. 1. Sample pretreatment and ICP-MS analysis process. Biological tissues and fluids collected from animals and/or humans were digested in an alkaline environment (pH ca. 15, 200 °C, 2 h). The resulting mixture was then stabilized by adding concentrated HNO_3. Then, 500 µl of the mixture were diluted in 4500 µl of ICP-MS diluent and injected into the spectrometer for the determination of silicon (Si) content.

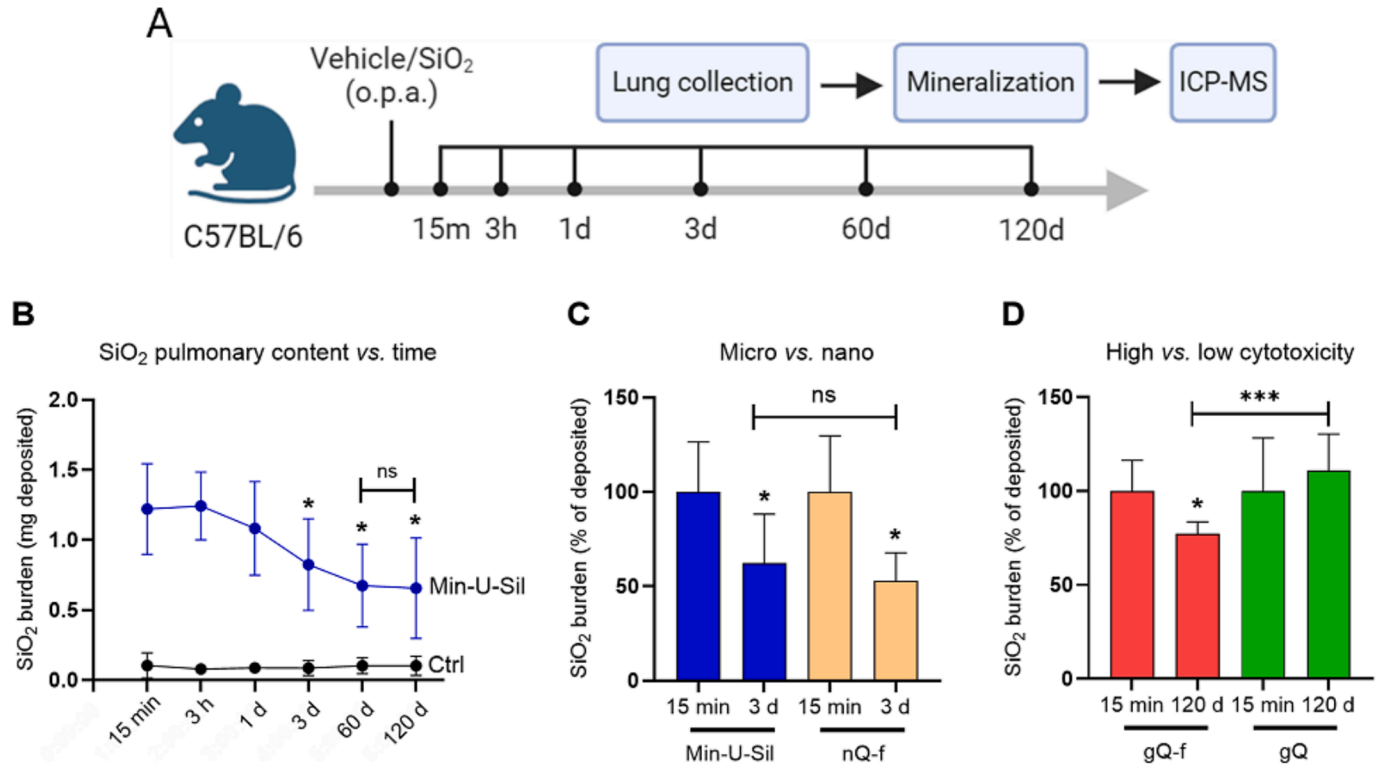

Fig. 2. Early and progressive clearance mechanisms partially remove crystalline silica deposited in the lungs. Changes of silica burden *vs.* time in the lungs of mice exposed to a set of different crystalline silica particles. (A) Experimental setup: animals were sacrificed 15 min, 3 h, 1 d, 3 d, 60 d or 120 d after particle exposure via oropharyngeal aspiration (o.p.a, 2.5 mg/mouse, 50 µl). Control animals were exposed to 0.9 % NaCl. Lungs were extracted and mineralized. Time-dependent crystalline silica burden was quantified by monitoring pulmonary Si content via ICP-MS analysis in the lungs of exposed mice. (B) Progressive decrease in the pulmonary content of Min-U-Sil particles due to particle translocation monitored 15 min, 3 h, 1, 3, 60, and 120 d after instillation (Ctrl and Min-U-Sil: n = 8/group per time interval). (C) Mice treated with nano-nanometric nQ-f crystalline silica do not show evident differences in the translocation amplitude when compared to animals treated with the same mass of micrometric Min-U-Sil 5 particles (Min-U-Sil and nQ-f: n = 8/group per time interval). (D) Mice treated with synthetic crystalline silica particles having different NFS content and contrasting toxic potentials (gQ-f: NFS-rich, high toxicity; gQ: NFS-poor, low toxicity) show silica particles are cleared from the lungs in a toxicity-dependent fashion (gQ-f and gQ: n = 8/group per time interval). One-way ANOVA with post-hoc Tukey's multiple comparisons test was applied to compare treated groups (3 h, 1 d, 3 d, 60 d, 120 d) *vs.* 15 min (panel B). Unpaired Student's *t*-test was applied to compare 15 min *vs.* 3 d and Min-U-Sil *vs* nQ-f (panel C) or 15 min *vs.* 120 d and gQ-f *vs.* gQ (panel D); ns: not significant, $^{*}P < 0.033$, $^{**}P < 0.002$, and $^{***}P < 0.001$.

3.2. Crystalline silica particles accumulate in different distal organs after early and late translocation

To detail particle migration in extrapulmonary target sites, we monitored crystalline silica accumulation in the liver, kidneys, mediastinal lymph nodes, spleen, and skin 15 min, 3 d and 120 d after Min-U-Sil 5 instillation. Time-dependent accumulation in extrapulmonary organs is expressed as the ratio calculated between the quantity of silica deposited in the lungs (Si levels, deposited dose at 15 min) and in the other organs at each time interval. As mentioned before, a progressive decrease in the pulmonary content was observed at 3 and 120 days (34 % and 45 % when compared to 15 min, respectively) (Fig. 3). This reduction paralleled particle accumulation in the liver (3 and 12 % at 3 and 120 d, respectively) and kidneys (1 and 2 % at 3 and 120 d) (Fig. 3). Significant particle accumulation was also evidenced 120 d post administration in the two distal immune organs lymph nodes (12 % of the deposited dose) and spleen (1.8 %). At this late time interval, particle accumulation in skin specimens was also detected (1.7 %). Interestingly, these three compartments (lymph nodes, spleen, and skin) were not impacted by early particle translocation occurring from 15 min to 3 d.

To support ICP-MS findings, we investigated particle burden by microscopy in the impacted organs (lungs, liver, kidneys, lymph nodes, spleen, and abdominal skin). Representative bright field (BF) and polarized microscopy (PL) images collected at day 120 are shown in Fig. 4 and in the Supplementary materials (Fig. S3). When compared to control lungs (Fig. 4A), H&E-stained slides first confirmed a substantial disorganization of the pulmonary tissue characterized by large nodules following silica exposure (Fig. 4C). No major tissue damage was observed in the liver (Fig. 4E-4G), kidneys (Fig. 4I-4 K), lymph nodes (Fig. 4M-4O), spleen (Fig. 4Q-4S), and skin (Fig. 4T-4 W). In line with ICP-MS data, PL imaging confirmed the presence of crystalline silica particles retained in the lungs of silica-treated mice (Fig. 4D). In addition, the significant presence of particles in the liver was evidenced (Fig. 4H). As expected, variable silica accumulation was also observed in kidneys (especially in proximity of the glomeruli) (Fig. 4L), mediastinal lymph nodes (Fig. 4P), spleen (Fig. 4T), and abdominal skin (in particular, throughout the dermis and subcutaneous tissue, Fig. 4X) of exposed mice.

Overall, these observations suggest that extrapulmonary particle relocation is a dynamic, biphasic, and time-dependent process. An early-phase mechanism drives the rapid distribution and accumulation of particles in the liver and kidneys, while a later-phase process contributes to their delayed relocation into immune organs and skin.

3.3. Silicon level increase in blood and urine as a hallmark of early and late particle translocation in treated mice

Aiming to clarify the routes leading to extrapulmonary silica distribution, we next quantified Si levels in different body fluids (including urine, blood, and plasma) collected from Min-U-Sil 5 silica-treated mice at different time points (15 min, 1 d, 3 d and 120 d, Fig. 5). Different patterns were observed, according to the considered fluid. Crystalline

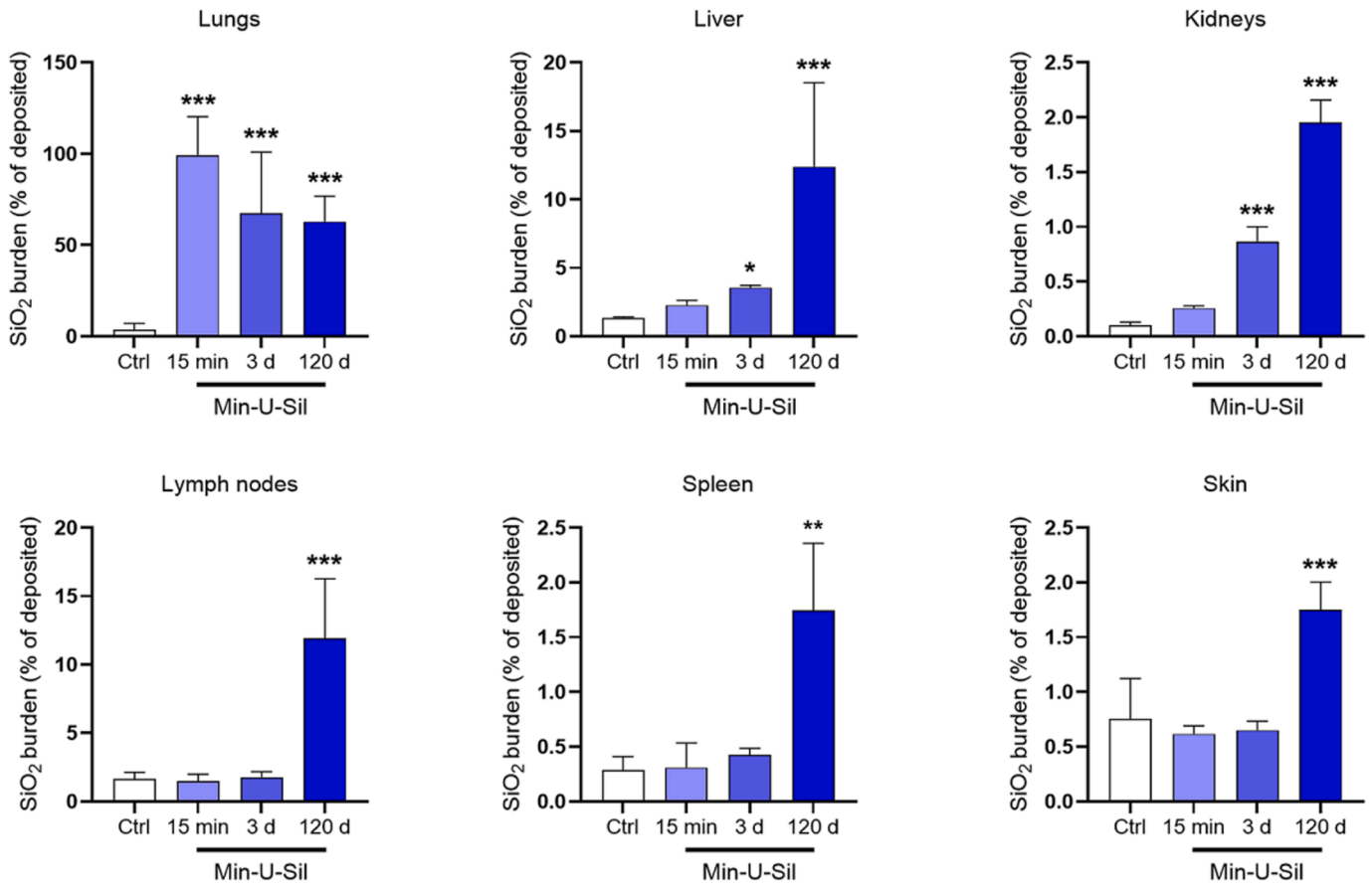

Fig. 3. Time-dependent biodistribution mechanisms contribute to particle translocation from the lungs to distal organs. Crystalline silica short- (15 min and 3 d) and long-term (120 d) biodistribution following Min-U-Sil 5 pulmonary administration (o.p.a., 2.5 mg /mouse) was evaluated by monitoring Si content via ICP-MS analysis in a set of distal organs, including liver, kidneys, mediastinal lymph nodes, spleen, and abdominal skin (Ctrl: n = 24 including control samples from the 3 time intervals considered; Min-U-Sil: 15 min, n = 8; 3 d, n = 8; 120 d, n = 8). Short- and long-term accumulation was detected in liver and, to a small extent, kidneys. Long-term translocation of silica, but not early, was additionally observed in lymph nodes, spleen, and abdominal skin. Accumulation in distal organs occurred in parallel with particle removal from the lungs. One-way ANOVA with post-hoc Tukey's multiple comparisons test was applied to compare treated groups (15 min, 3 d, 120 d) *vs.* Ctrl; $*P < 0.033$, $**P < 0.002$, and $***P < 0.001$.

silica exposure resulted in a 2-fold increase in urine Si level with respect to controls at day 120 (Fig. 5). Conversely, no early variation was evidenced at 3 d, indicating accumulation in urine and clearance as a late-occurring event (Fig. 5). In contrast, an early Si increase was detected in the blood 1 and 3 days after the treatment (Fig. 5). At 120 d, blood Si content was undistinguishable from control animals, suggesting the early (not late) accumulation of silica in the blood circulation after pulmonary deposition (Fig. 5). Unchanged Si content was measured in the plasma of exposed animals among the different time points evaluated (Fig. 5). These observations highlight the pivotal role of blood circulation in the early extrapulmonary biodistribution of silica and reveal delayed renal clearance in treated mice. Furthermore, the results suggest that Si levels in blood and urine could serve as potential biomarkers for tracing crystalline silica exposure.

3.4. The level of silicon in urine and blood of exposed workers represents an effective biomarker to assess human exposure to crystalline silica

To test Si level as a possible biomarker of occupational exposure to silica dust, we compared Si concentration in the fluids previously described (urine, blood, and plasma) collected from a mine worker group and a group unexposed to silica (Fig. 6). Consistent with the result of animal experiments, we observed that the median (Fig. 6A, red line) urine Si in the workers was significantly higher than that of the control group (ca. 15,000 *vs.* 5,000 μg/l). Similarly, quantification in blood showed a higher amount of Si in workers when compared to controls (Fig. 6B). No difference was observed in plasma Si from controls and mine workers (Fig. 6C). To corroborate these results, Si was further quantified in urine samples (n = 61) collected from subjects working in the porcelain industry (Porcelain workers). This industrial context is characterized by the potential exposure of workers to silica, especially in the form of quartz (Birk et al., 2010; Molinari et al., 2024). Consistent with the findings in miners, porcelain workers exhibited a significant increase in urinary Si with respect to the control group (Fig. 6D). These results indicate that systemic distribution of silica resulting from inhalational exposure occurs in humans and leads to an increase in both urine and blood silicon. Si concentration in urine and/or blood may thus serve as biomarker for assessing the occupational exposure to silica particles, providing insights into both current and past exposure levels.

4. Discussion

Case studies suggest that respirable crystalline silica (RCS) particles deposited in the lungs following inhalation impact distal organs because of particle extrapulmonary migration and relocation (Guarnieri et al., 2019; Steenland et al., 2002; Carreno Hernandez et al., 2019). Although different mechanisms have been proposed, the exact pathway driving the internal distribution of particles from the lungs to extrapulmonary organs remains unclear and not yet quantified (Nakane, 2012; Wang et al., 2022).

In vivo studies represent suitable experimental approaches to quantify the extrapulmonary distribution of particles following

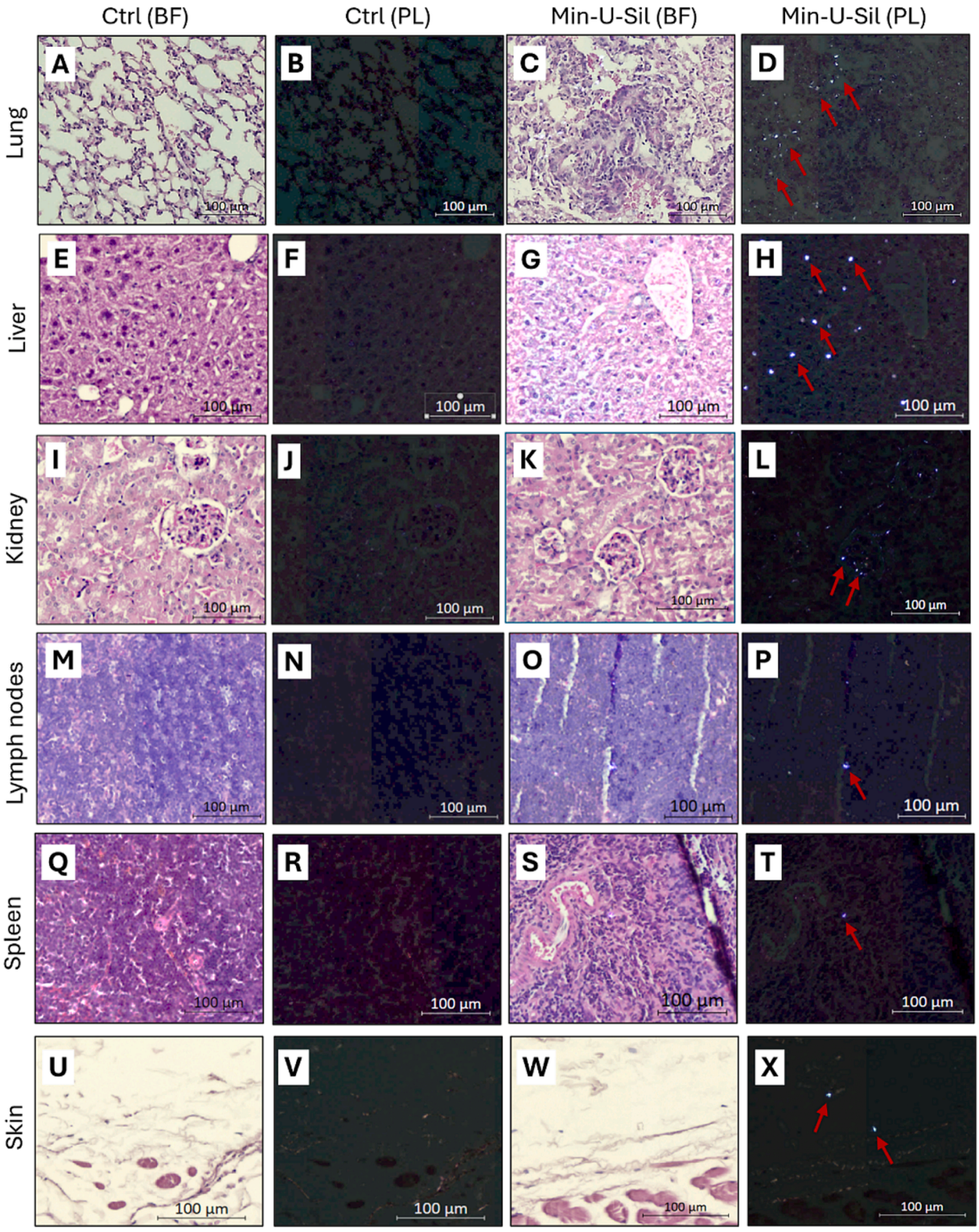

Fig. 4. Imaging evidenced particle bioaccumulation in distal organs of silica-exposed mice as the result of extrapulmonary translocation processes. Representative images of H&E-stained slides (5 µm) in bright field (BF) and polarized light (PL) of organ specimens obtained from saline-treated mice (Ctrl, n = 6) and mice exposed 120 days to 2.5 mg of crystalline silica particles (Min-U-Sil, n = 6). (A-D) lung, (E-H) liver, (I-L) kidney, (M−P) mediastinal lymph nodes, (Q-T) spleen, (U-X) skin. Crystalline silica particles deposited in the tissue are pointed by red arrows. (For interpretation of the references to colour in this figure legend, the reader is referred to the web version of this article.)

deposition in the lungs. By using an innovative quantitative methodology based on ICP-MS measuring the level of silicon (Si), we found that a significant fraction of crystalline silica settled in the lungs of mice treated with a single instillation via o.p.a., translocated and accumulated in specific distal organs including liver (12 % of the particle dose initially deposited in the lungs), kidneys (2 %), mediastinal lymph nodes (12 %), spleen (1.8 %), and abdominal skin (1.7 %). The biodistribution of silica particles in extrapulmonary targets was further

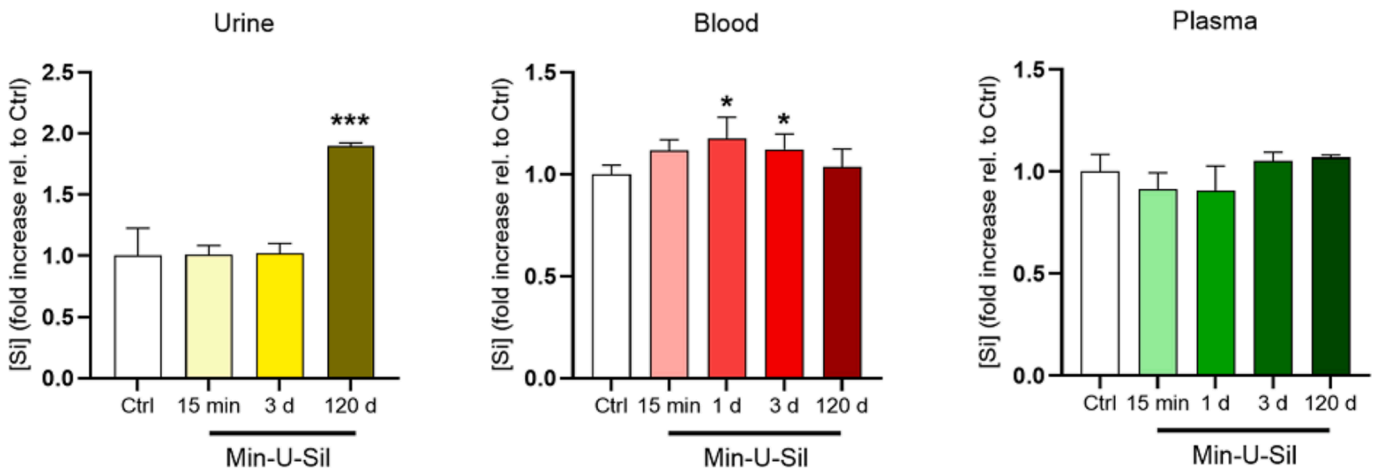

Fig. 5. Silicon level in urine and blood show time-dependent increase following silica pulmonary exposure. Changes in silicon (Si) concentration in urine, blood and plasma samples collected from animals unexposed (Ctrl; urine: n = 24, blood and plasma: n = 32) or exposed to Min-U-Sil crystalline silica (2.5 mg/mouse; sample size: n = 8 per each time interval were measured 15 min, 1 d, 3 d, and 120 d after crystalline silica exposure via ICP-MS analysis. Control animals were treated with 0.9 % NaCl. A significant increase in urine Si was observed 120 d after the exposure. Early (1 d and 3 d) Si level increase was found in the blood. No significant time-dependent variation was detected in plasma. $^{*}P < 0.033$, $^{**}P < 0.002$, and $^{***}P < 0.001$ *vs.* Ctrl unexposed to silica. (One-way ANOVA with Tukey's multiple comparisons test).

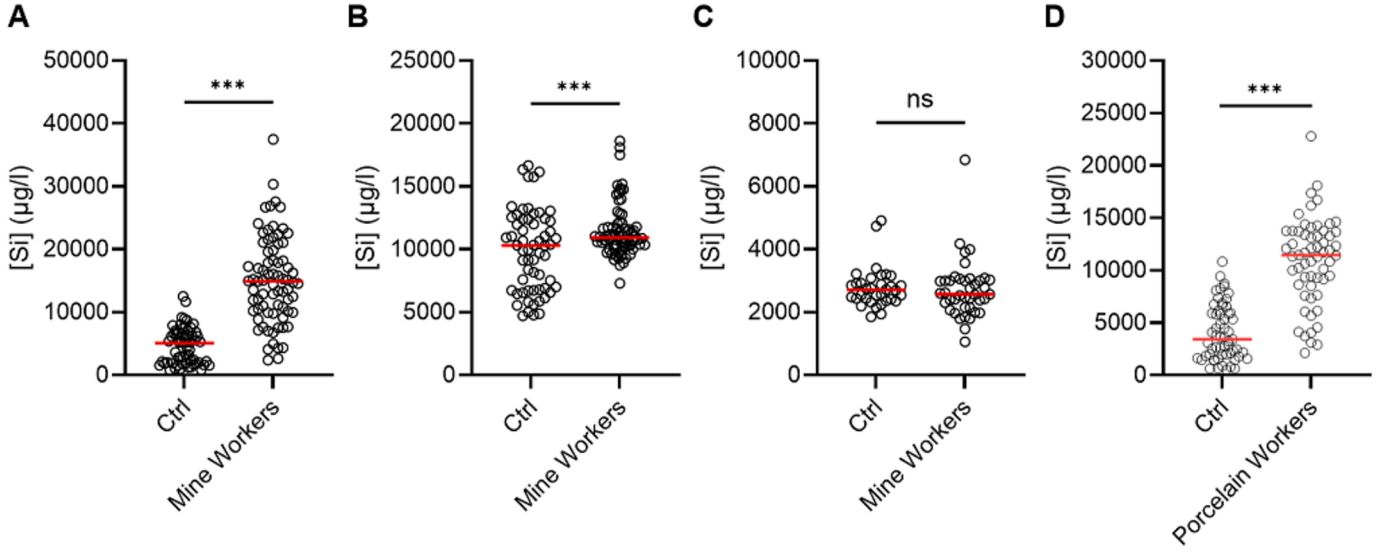

Fig. 6. Biomonitoring of silica exposure in workers by quantifying urine and blood Si levels. The concentration of Si in body fluids (urine, blood, and plasma) collected from nonexposed (Ctrl) or exposed volunteers (Mine Workers, Porcelain Workers) was measured via ICP-MS. (A) Urine Si of Ctrl and Mine workers. (B) Blood Si of Ctrl and Mine workers. (C) Plasma Si of Ctrl and Mine workers. (D) Urine Si of Ctrl and Porcelain workers. Red line: median. Each circle represents one volunteer. ns: not significant. $^{***}P < 0.001$ *vs.* Ctrl unexposed to crystalline silica (unpaired Student's *t*-test). (For interpretation of the references to colour in this figure legend, the reader is referred to the web version of this article.)

confirmed by imaging via polarized microscopy. This technique is commonly used to detect crystalline silica localized in lung sections collected from exposed murine models (Arras et al., 2001; Satpathy et al., 2015).

The accumulation rate in distal organs was not uniform over time. Specifically, the liver and kidneys exhibited early translocation, occurring within 3 days of particle administration. This rapid extrapulmonary accumulation suggests the activation of bloodstream-dependent translocation mechanisms, which facilitate the distribution of a primary fraction of toxic particles rich in nearly free silanols (NFS) to early target organs. The marked difference in pulmonary retention between NFS-poor and NFS-rich silica may be due to the latter's ability to enhance the permeabilization of the alveolar-capillary barrier (Pavan et al., 2024), promoting the migration of NFS-rich toxic particles into the bloodstream. In contrast, nonreactive NFS-poor particles, which do not induce harmful tissue responses, remained in the lungs. This finding supports the crucial role of particle toxicity (influenced by surface chemistry) in governing lung clearance and extrapulmonary distribution. Notably, our results suggest that particle size is not a principal determinant in the removal of crystalline silica from the lungs. Specifically, although the average hydrodynamic diameter of nQ-f is significantly smaller than that of Min-U-Sil 5 (refer to Table 1), no appreciable differences in pulmonary clearance were observed between the two crystalline dusts. Nonetheless, we cannot completely rule out the potential influence of particle size on the systemic distribution and subsequent bioaccumulation of silica in extrapulmonary tissues. Further mechanistic studies employing silica preparations with broader and well-defined particle size distributions are warranted.

The liver and the kidneys have a high blood supply relative to their weight (Racanelli and Rehermann, 2006). The liver, a key filtration

organ, has been shown to purify blood of administered particles, aided by blood-circulating Kupffer cells (Zhang et al., 2016). The rapid accumulation of particles in these organs, due to bloodstream distribution, has been previously observed in a rat model (Brooking et al., 2001). We propose that NFS-reactive silica accumulated in the bloodstream is quickly distributed to the liver via the hepatic artery and/or portal vein. A similar mechanism, likely driven by the renal artery, may account for silica accumulation in the kidneys after retention in the glomeruli. This process involves damage to the air-blood barrier, translocation to the capillary lumen, and passive accumulation in the well-perfused liver and kidneys (Leibrock et al., 2020; Leibrock et al., 2019; Singh et al., 2021). Notably, enhanced alveolar-capillary barrier permeability is a known early outcome of the pulmonary proinflammatory activity of toxic crystalline silica (Castranova et al., 2002; Inoue et al., 2009). The rapidity of this translocation suggests that phagocytosis by macrophages and/or endocytosis by epithelial/endothelial cells are unlikely mechanisms in steering the early extrapulmonary distribution of silica (Nemmar et al., 2002).

An additional fraction of toxic particles was distributed via the contribution of supplementary mechanisms to late-impacted organs including mediastinal lymph nodes, spleen, and abdominal skin (Fig. S3 and S4, Supplementary materials). This delayed process probably implicates active phagocytosis and distribution in draining lymph nodes by alveolar macrophages and dendritic cells via the lymphatic vessels (Manolova et al., 2008; Blank et al., 2013). This immuno-mediated clearance is potentially based on specific subclasses of surface receptors including the scavenger receptor MARCO (macrophage receptor with collagenous structure) and/or the pattern recognition receptor (PRR) CD206. Indeed, these protein molecules were proposed as responsible for silica sensing and internalization in antigen-presenting cells (Hammad and Lambrecht, 2007; Feray et al., 2021; Hamilton et al., 2006; Gallud et al., 2017; Huaux, 2018). The translocation of particles to draining lymph nodes may also be a direct consequence of silica-associated lung epithelial injury, resulting in a compromised tissue integrity and increased accumulation of particles in the lymphatic vessels (Adamson and Prieditis, 1998; Wei et al., 2012). Despite some studies suggest that the transport through the lymphatic system may also result in splenic accumulation upon inhalation, the influence of the bloodstream in silica biodistribution process to the spleen should be considered (Nakane, 2012; Wei et al., 2012; Mitchell et al., 2007). Overall, our data support the possibility that target immune organs, including spleen and lymph nodes, may be largely impacted by direct or indirect adverse toxic effects (including proinflammatory responses) associated with the chronic accumulation of NFS-rich toxic particles (Chandrasekar et al., 2024). Such effects could ultimately trigger autoimmune/autoinflammatory responses compromising crucial physiological immune functions (Parks et al., 1999; Ural et al., 2022; Zhang et al., 2024). In line with our results, rats treated with crystalline silica in the form of alpha-cristobalite or quartz, showed particle migration in mediastinal lymph nodes after administration in the lungs via pulmonary deposition (Absher et al., 1992; Kobayashi et al., 2023). Silica ultimately accumulated in urine, in accordance with a previous study carried out in the rat (Sasai et al., 2022). Since crystalline silica dissolution in vivo is negligible because of its intrinsic physico-chemical properties, our data suggest the presence of particles in urine of exposed mice as the result of late renal clearance. The presence of silica or high Si levels in body fluids (urine and blood serum) collected from individuals occupationally exposed to crystalline silica has been reported in previous studies (Ferri et al., 2018; Wang et al., 2021; Hussein et al., 2023). Accordingly, our data revealed significant urine and blood Si increase in silica-exposed workers, when compared to unexposed controls. This supports the potential role of blood/urine Si as a general tracer for silica exposure. In addition, these results, corroborated by the observations in the mouse, suggest the bloodstream as a key player in the process of systemic biodistribution following particle exposure and reinforce silica accumulation in urine following extrapulmonary distribution in the kidneys. The body of evidence for a causal relationship between exposure to crystalline silica and kidney disease is continuously growing, despite the nature of this association is unclear (Mohner et al., 2017; Vupputuri et al., 2012; Fenwick and Main, 2000). Our data suggest that silica-induced nephrotoxicity could be the direct consequence of the deposition of reactive particles in the kidney, in line with observations reported in the literature (Vupputuri et al., 2012; Steenland et al., 2002; ATSDR, 2019). By taking advantage of our animal data, these observations lead us to propose blood Si as a function of current exposure to crystalline silica, and urine Si as a biomarker of past exposure.

This study presents some limitations. We recognize that different species-specific features between mice and humans including anatomy and geometry of airways, respiratory physiology, cell subtypes, pulmonary mucus compositions, biochemical mechanisms, and metabolic processes, modify the deposition and retention of inhaled particles in the respiratory tract (Movia et al., 2020; Asgharian et al., 2014). A recent computational study pointed out a higher clearance rate for murine lungs, when compared to the human lung (Kolanjiyil et al., 2019). However, the effectiveness of models developed in rodents in predicting the pulmonary deposition, biodistribution and clearance of inhaled particles in humans, in particular for fine (< 2.5 μm) and submicrometer (< 1 μm) objects, has been suggested by different studies (Gakis et al., 2022; Han et al., 2023). Another possible criticism of our study regards oropharyngeal aspiration (o.p.a.) as the selected particle administration route (De Vooght et al., 2009). This bolus-type approach does not represent the physiological mode of exposure to airborne particles, and accidental particle ingestion may occur (Kunda et al., 2018). In this context, we did not observe short- or long-term silica accumulation in stomach or gut (Fig. S2, Supplementary materials). The administration route is known to affect pulmonary particle deposition and modulate the pattern of cells recruited in the lungs (Yisrael et al., 2023; Lazaridis, 2023). Nevertheless o.p.a., which allows to instill a precise dose of particles in the airways of treated animals, presents additional advantages when compared to other administration routes, including more efficients particle distribution and penetration in the lungs following deposition, and great reproducibility among the animals (De Vooght et al., 2009; Lakatos et al., 2006). Inhalation experiments would potentially simulate exposure conditions more realistically than o.p.a. However, inhalation exposure presents several drawbacks such as animal discomfort, potential issues with the administrated dose, and possible sample contamination (Pauluhn, 2005; Song et al., 2021).

An additional limitation of our study regards quantitative relationship between the overall crystalline silica exposure and the level of silica (or silicon) in urine (ATSDR, 2019). This aspect includes the event of external contamination during sample collection, which could ultimately result in data misinterpretation when monitoring urine Si (Durand-Moreau, 2023). Furthermore, workers from the same mining site can be exposed to several sources of silicon in addition to crystalline silica, such as different groups of silicate minerals (i.e., feldspars, clay). Therefore, some uncertainty in proving crystalline silica as the only responsible for blood/urine Si increase may exist. Interestingly, urine Si recently measured in urine collected from a cohort of RCS-unexposed individuals from China, well matches our control group (Wang et al., 2021). This suggests that confounding factors (i.e., dietary intake and other environmental sources of Si) are well represented in our unexposed population. Because of comparable geographical location, age distribution, and smoking habits among the unexposed and exposed subjects considered in this study, we assume that the increased Si levels (and not the overall amount) detected in the blood and urine of miners and porcelain workers are due to occupational silica exposure. The quantitative evaluation of workers' silica external exposure levels via environmental monitoring approaches (external dose) would assist in solving these constraints, certifying the effective reliability of urine Si as an exposure biomarker.

International agencies have set occupational exposure limit values

for RCS (0.1 mg/m^3 in Europe, 0.05 mg/m^3 in the United States) to ensure workers' protection. However, because of the intrinsic physico-chemical properties of crystalline silica (e.g., poor solubility), the abundance of Si in the environment, and the technical difficulties affecting the sensitivity of common analytical methods in measuring Si in biological matrices, no biological limit values have been recommended so far. Therefore, the need for reliable biomonitoring strategies is compelling. Our study may assist national and international regulatory agencies in proposing innovative biomonitoring strategies and harmonizing exposure assessment protocols, to standardize safety policies and optimize uncertainty factors (Dankovic et al., 2015). The comparison of Si levels in body fluids from exposed subjects with those of patients diagnosed with silicosis and/or other RCS-related pathologies, in association with early clinical biomarkers, may potentially contribute in identifying individuals with higher risk of developing occupational diseases (Calutu et al., 2022). Our findings can be extended to communities exposed to other silica-based materials including amorphous silicas and silicate mineral dust, which may represent an environmental hazard for non-occupational populations.

5. Conclusions

Our study unveils novel insights into the biokinetic mechanisms underlining the extrapulmonary biodistribution of crystalline silica, following deposition in the lungs. By this process, toxic silica progressively removed from the lungs via early or late processes reach and ultimately accumulate into different target extrapulmonary compartments, before being excreted in urine. When prolonged over time, this biodistribution/accumulation mechanism may lead to organ dysfunctions due to direct or indirect effects associated with toxic particle overloading. In the context of silica exposure biomonitoring, silicon level in urine and/or blood represents a potential candidate to serve as biomarker of current and past crystalline silica exposure. Future research should aim to set a quantitative threshold to determine excessive exposure, possibly related to the onset of silica-induced local and systemic pathologies.

CRediT authorship contribution statement

Riccardo Leinardi: Writing – original draft, Visualization, Formal analysis, Data curation. **Chiara Longo Sanchez-Calero:** Investigation, Formal analysis, Data curation. **Saloua Ibouraadaten:** Investigation. **Francine Uwambayinema:** Investigation. **Yousof Yakoub:** Investigation. **Cristina Pavan:** Writing – review & editing, Resources. **Rani Claus:** Resources, Investigation. **Frauke Lemaire:** Resources, Investigation. **Steven Ronsmans:** Writing – review & editing, Validation, Methodology. **Manosij Ghosh:** Writing – review & editing, Validation, Methodology. **Lénárd Farczádi:** Resources. **Horatiu Moldovan:** Resources, Conceptualization. **Jeroen A.J. Vanoirbeek:** Investigation. **Francesco Turci:** Writing – review & editing, Resources. **Peter H.M. Hoet:** Investigation. **François Huaux:** Writing – review & editing, Supervision, Funding acquisition, Data curation, Conceptualization.

Ethics approval and consent to participate

Animal studies were approved by the Institutional Animal Care and Use Committee (EEC n°86/609, LA1230312 and 2022/UCL/MD/019), respectively.

Funding

This work was supported by the « Actions de Recherche Concertées », Fédération Wallonie-Bruxelles (ARC 19/24-098, CYTAID) and « European Union's Horizon 2020 research and innovation programme » (874707, EXIMIOUS). FH is a Senior Research Associate with the FNRS, Belgium.

Declaration of competing interest

The authors declare that they have no known competing financial interests or personal relationships that could have appeared to influence the work reported in this paper.

Acknowledgements

Not applicable.

Appendix A. Supplementary data

Supplementary data to this article can be found online at https://doi.org/10.1016/j.envint.2025.109473.

Data availability

Data will be made available on request.

References

IARC, 2012. Arsenic, metals, fibres, and dusts, IARC Monogr Eval Carcinog Risks Hum 100 (Pt C), 11–465.
Sato, T., Shimosato, T., Klinman, D.M., 2018. *Silicosis and lung cancer: current perspectives.* Lung Cancer (auckl) 9, 91–101.
Hoy, R.F., Chambers, D.C., 2020. *Silica-related diseases in the modern world.* Allergy 75 (11), 2805–2817.
Pavan, C., Santalucia, R., Leinardi, R., Fabbiani, M., Yakoub, Y., Uwambayinema, F., Ugliengo, P., Tomatis, M., Martra, G., Turci, F., Lison, D., Fubini, B., 2020. *Nearly free surface silanols are the critical molecular moieties that initiate the toxicity of silica particles.* Proc Natl Acad Sci U S A 117 (45), 27836–27846.
Leinardi, R., Pochet, A., Uwambayinema, F., Yakoub, Y., Quesniaux, V., Ryffel, B., Broz, P., Pavan, C., Huaux, F., 2023. *Gasdermin D membrane pores orchestrate IL-1alpha secretion from necrotic macrophages after NFS-rich silica exposure.* Arch Toxicol.
Pavan, C., Santalucia, R., Escolano-Casado, G., Ugliengo, P., Mino, L., Turci, F., 2023. *Physico-Chemical Approaches to Investigate Surface Hydroxyls as Determinants of Molecular Initiating Events in Oxide Particle Toxicity.* Int J Mol Sci 24 (14).
Pavan, C., Leinardi, R., Benhida, A., Ibouraadaten, S., Yakoub, Y., Brule, S.V.D., Lison, D., Turci, F., Huaux, F., 2024. *Short- and long-term pathologic responses to quartz are induced by nearly free silanols formed during crystal fracturing.* Part Fibre Toxicol 21 (1), 52.
Osorio, A.M., Thun, M.J., Novak, R.F., Van Cura, E.J., Avner, E.D., 1987. *Silica and glomerulonephritis: case report and review of the literature.* Am J Kidney Dis 9 (3), 224–230.
Mohner, M., Pohrt, A., Gellissen, J., 2017. *Occupational exposure to respirable crystalline silica and chronic non-malignant renal disease: systematic review and meta-analysis.* Int Arch Occup Environ Health 90 (7), 555–574.
Guarnieri, G., Bizzotto, R., Gottardo, O., Velo, E., Cassaro, M., Vio, S., Putzu, M.G., Rossi, F., Zuliani, P., Liviero, F., Mason, P., Maestrelli, P., 2019. *Multiorgan accelerated silicosis misdiagnosed as sarcoidosis in two workers exposed to quartz conglomerate dust.* Occup Environ Med 76 (3), 178–180.
Marinaccio, A., Scarselli, A., Gorini, G., Chellini, E., Mastrantonio, M., Uccelli, R., Altavista, P., Pirastu, R., Merlo, D.F., Nesti, M., 2006. *Retrospective mortality cohort study of Italian workers compensated for silicosis.* Occup Environ Med 63 (11), 762–765.
Ibrahim, K.S., Ahmed, S.B., Amer, N.M., 2011. *Study of kidney dysfunction in non-silicotic Egyptian workers.* Int J Hyg Environ Health 214 (1), 53–58.
Vupputuri, S., Parks, C.G., Nylander-French, L.A., Owen-Smith, A., Hogan, S.L., Sandler, D.P., 2012. *Occupational silica exposure and chronic kidney disease.* Ren Fail 34 (1), 40–46.
Rubio-Rivas, M., Moreno, R., Corbella, X., 2017. *Occupational and environmental scleroderma. Systematic Review and Meta-Analysis.* Clin Rheumatol 36 (3), 569–582.
Parks, C.G., Cooper, G.S., Nylander-French, L.A., Sanderson, W.T., Dement, J.M., Cohen, P.L., Dooley, M.A., Treadwell, E.L., St Clair, E.W., Gilkeson, G.S., Hoppin, J. A., Savitz, D.A., 2002. *Occupational exposure to crystalline silica and risk of systemic lupus erythematosus: a population-based, case-control study in the southeastern United States.* Arthritis Rheum 46 (7), 1840–1850.
Ferri, C., Artoni, E., Sighinolfi, G.L., Luppi, F., Zelent, G., Colaci, M., Giuggioli, D., 2018. *High serum levels of silica nanoparticles in systemic sclerosis patients with occupational exposure: Possible pathogenetic role in disease phenotypes.* Semin Arthritis Rheum 48 (3), 475–481.
Aguila, L.A., da Silva, H.C., Medeiros-Ribeiro, A.C., Bunjes, B.G., Luppino-Assad, A.P., Sampaio-Barros, P.D., 2021. *Is exposure to environmental factors associated with a characteristic clinical and laboratory profile in systemic sclerosis? A Retrospective Analysis.* Rheumatol Int 41 (6), 1143–1150.
Boudigaard, S.H., Schlünssen, V., Vestergaard, J.M., Søndergaard, K., Torén, K., Peters, S., Kromhout, H., Kolstad, H.A., 2021. *Occupational exposure to respirable crystalline silica and risk of autoimmune rheumatic diseases: a nationwide cohort study.* Int J Epidemiol 50 (4), 1213–1226.

Morotti, A., Sollaku, I., Franceschini, F., Cavazzana, I., Fredi, M., Sala, E., De Palma, G., 2022. *Systematic Review and Meta-analysis on the Association of Occupational Exposure to Free Crystalline Silica and Rheumatoid Arthritis*. Clin Rev Allergy Immunol 62 (2), 333–345.
De Decker, E., Vanthuyne, M., Blockmans, D., Houssiau, F., Lenaerts, J., Westhovens, R., Nemery, B., De Langhe, E., 2018. *High prevalence of occupational exposure to solvents or silica in male systemic sclerosis patients: a Belgian cohort analysis*. Clin Rheumatol 37 (7), 1977–1982.
Parks, C.G., Conrad, K., Cooper, G.S., 1999. *Occupational exposure to crystalline silica and autoimmune disease*. Environ Health Perspect 107 Suppl 5(Suppl 5), 793–802.
Giles, R.D., Sturgill, B.C., Suratt, P.M., Bolton, W.K., 1978. *Massive proteinuria and acute renal failure in a patient with acute silicoproteinosis*. Am J Med 64 (2), 336–342.
Nakane, H., 2012. *Translocation of particles deposited in the respiratory system: a systematic review and statistical analysis*. Environ Health Prev Med 17 (4), 263–274.
Stuart, B.O., 1984. *Deposition and clearance of inhaled particles*. Environ Health Perspect 55, 369–390.
Wang, W., Lin, Y., Yang, H., Ling, W., Liu, L., Zhang, W., Lu, D., Liu, Q., Jiang, G., 2022. *Internal Exposure and Distribution of Airborne Fine Particles in the Human Body: Methodology, Current Understandings, and Research Needs*. Environ Sci Technol 56 (11), 6857–6869.
Kuempel, E.D., Sweeney, L.M., Morris, J.B., Jarabek, A.M., 2015. *Advances in Inhalation Dosimetry Models and Methods for Occupational Risk Assessment and Exposure Limit Derivation*. J Occup Environ Hyg 12 Suppl 1(sup1), S18–S40.
Qiu, J., Ma, J., Dong, Z., Ren, Q., Shan, Q., Liu, J., Gao, M., Liu, G., Zhang, S., Qu, G., Jiang, G., Liu, S., 2024. *Lung megakaryocytes engulf inhaled airborne particles to promote intrapulmonary inflammation and extrapulmonary distribution*. Nat Commun 15 (1), 7396.
Leese, E., Staff, J.F., Carolan, V.A., Morton, J., 2017. *Exhaled Breath Condensate: A Novel Matrix for Biological Monitoring to Assess Occupational Exposure to Respirable Crystalline Silica*. Ann Work Expo Health 61 (7), 902–906.
Kirkpatrick, J.J., Enion, D.S., Burd, D.A., 1995. *Hydrofluoric acid burns: a review*. Burns 21 (7), 483–493.
Wang, X., Zhang, Y., Ni, L., You, C., Ye, C., Jiang, R., Liu, L., Liu, J., Han, C., 2014. *A review of treatment strategies for hydrofluoric acid burns: current status and future prospects*. Burns 40 (8), 1447–1457.
Cai, H., Jiang, P., Jin, L., Hu, J., 2008. *Microwave enhanced alkaline digestion of silicate samples for determination of Fe2O3*. Talanta 77 (2), 800–803.
Bossert, D., Urban, D.A., Maceroni, M., Ackermann-Hirschi, L., Haeni, L., Yajan, P., Spuch-Calvar, M., Rothen-Rutishauser, B., Rodriguez-Lorenzo, L., Petri-Fink, A., Schwab, F., 2019. *A hydrofluoric acid-free method to dissolve and quantify silica nanoparticles in aqueous and solid matrices*. Sci Rep 9 (1), 7938.
Pastero, L., Turci, F., Leinardi, R., Pavan, C., Monopoli, M., 2016. *Synthesis of α-Quartz with Controlled Properties for the Investigation of the Molecular Determinants in Silica Toxicology*. Crystal Growth & Design 16 (4), 10.
Bellomo, C., Pavan, C., Fiore, G., Escolano-Casado, G., Mino, L., Turci, F., 2022. *Top-Down Preparation of Nanoquartz for Toxicological Investigations*. Int J Mol Sci 23 (23).
IARC, *IARC Working Group on the Evaluation of Carcinogenic Risks to Humans: Silica, Some Silicates, Coal Dust and Para-Aramid Fibrils. Lyon, 15-22 October 1996*. IARC Monogr Eval Carcinog Risks Hum, 1997. **68**: p. 1-475.
Pavan, C., Escolano-Casado, G., Bellomo, C., Canana, S., Tomatis, M., Leinardi, R., Mino, L., Turci, F., 2022. *Nearly free silanols drive the interaction of crystalline silica polymorphs with membranes: Implications for mineral toxicity*. Front Chem 10, 1092221.
Leinardi, R., Pavan, C., Yedavally, H., Tomatis, M., Salvati, A., Turci, F., 2020. *Cytotoxicity of fractured quartz on THP-1 human macrophages: role of the membranolytic activity of quartz and phagolysosome destabilization*. Arch Toxicol 94 (9), 2981–2995.
Huaux, F., Arras, M., Tomasi, D., Barbarin, V., Delos, M., Coutelier, J.P., Vink, A., Phan, S.H., Renauld, J.C., Lison, D., 2002. *A profibrotic function of IL-12p40 in experimental pulmonary fibrosis*. J Immunol 169 (5), 2653–2661.
Giordano, G., van den Brule, S., Lo Re, S., Triqueneaux, P., Uwambayinema, F., Yakoub, Y., Couillin, I., Ryffel, B., Michiels, T., Renauld, J.C., Lison, D., Huaux, F., 2010. *Type I interferon signaling contributes to chronic inflammation in a murine model of silicosis*. Toxicol Sci 116 (2), 682–692.
Hoet, P., Jacquerye, C., Deumer, G., Lison, D., Haufroid, V., 2013. *Reference values and upper reference limits for 26 trace elements in the urine of adults living in Belgium*. Clin Chem Lab Med 51 (4), 839–849.
Hoet, P., Jacquerye, C., Deumer, G., Lison, D., Haufroid, V., 2021. *Reference values of trace elements in blood and/or plasma in adults living in Belgium*. Clin Chem Lab Med 59 (4), 729–742.
Rabolli, V., Badissi, A.A., Devosse, R., Uwambayinema, F., Yakoub, Y., Palmai-Pallag, M., Lebrun, A., De Gussem, V., Couillin, I., Ryffel, B., Marbaix, E., Lison, D., Huaux, F., 2014. *The alarmin IL-1alpha is a master cytokine in acute lung inflammation induced by silica micro- and nanoparticles*. Part Fibre Toxicol 11, 69.
Huang, H., Chen, M., Liu, F., Wu, H., Wang, J., Chen, J., Liu, M., Li, X., 2019. *N-acetylcysteine tiherapeutically protects against pulmonary fibrosis in a mouse model of silicosis*. Biosci Rep 39 (7).
Nemmar, A., Vanbilloen, H., Hoylaerts, M.F., Hoet, P.H., Verbruggen, A., Nemery, B., 2001. *Passage of intratracheally instilled ultrafine particles from the lung into the systemic circulation in hamster*. Am J Respir Crit Care Med 164 (9), 1665–1668.
Choi, H.S., Ashitate, Y., Lee, J.H., Kim, S.H., Matsui, A., Insin, N., Bawendi, M.G., Semmler-Behnke, M., Frangioni, J.V., Tsuda, A., 2010. *Rapid translocation of nanoparticles from the lung airspaces to the body*. Nat Biotechnol 28 (12), 1300–1303.
Liu, Q., Guan, J., Qin, L., Zhang, X., Mao, S., 2020. *Physicochemical properties affecting the fate of nanoparticles in pulmonary drug delivery*. Drug Discov Today 25 (1), 150–159.
Pavan, C., Sydor, M.J., Bellomo, C., Leinardi, R., Canana, S., Kendall, R.L., Rebba, E., Corno, M., Ugliengo, P., Mino, L., Holian, A., Turci, F., 2022. *Molecular recognition between membrane epitopes and nearly free surface silanols explains silica membranolytic activity*. Colloids Surf B Biointerfaces 217, 112625.
Birk, T., Guldner, K., Mundt, K.A., Dahmann, D., Adams, R.C., Parsons, W., 2010. *Quantitative crystalline silica exposure assessment for a historical cohort epidemiologic study in the German porcelain industry*. J Occup Environ Hyg 7 (9), 516–528.
Molinari, C., Conte, S., Dondi, M., Zanelli, C., 2024. *Content of crystalline silica phases in porcelain stoneware*. Open Ceramics 19.
Steenland, K., Rosenman, K., Socie, E., Valiante, D., 2002. *Silicosis and end-stage renal disease*. Scand J Work Environ Health 28 (6), 439–442.
Carreno Hernandez, M.C., Garrido Paniagua, S., Colomes Iess, M., Guemra, M., 2019. *Accelerated silicosis with bone marrow, hepatic and splenic involvement in a patient with lung transplantation*. BMJ Case Rep 12 (12).
Arras, M., Huaux, F., Vink, A., Delos, M., Coutelier, J.P., Many, M.C., Barbarin, V., Renauld, J.C., Lison, D., 2001. *Interleukin-9 reduces lung fibrosis and type 2 immune polarization induced by silica particles in a murine model*. Am J Respir Cell Mol Biol 24 (4), 368–375.
Satpathy, S.R., Jala, V.R., Bodduluri, S.R., Krishnan, E., Hegde, B., Hoyle, G.W., Fraig, M., Luster, A.D., Haribabu, B., 2015. *Crystalline silica-induced leukotriene B4-dependent inflammation promotes lung tumour growth*. Nat Commun 6, 7064.
Racanelli, V., Rehermann, B., 2006. *The liver as an immunological organ*. Hepatology 43 (2 Suppl 1), S54–S62.
Zhang, Y.N., Poon, W., Tavares, A.J., McGilvray, I.D., Chan, W.C.W., 2016. *Nanoparticle-liver interactions: Cellular uptake and hepatobiliary elimination*. J Control Release 240, 332–348.
Brooking, J., Davis, S.S., Illum, L., 2001. *Transport of nanoparticles across the rat nasal mucosa*. J Drug Target 9 (4), 267–279.
Leibrock, L.B., Jungnickel, H., Tentschert, J., Katz, A., Toman, B., Petersen, E.J., Bierkandt, F.S., Singh, A.V., Laux, P., Luch, A., 2020. *Parametric Optimization of an Air-Liquid Interface System for Flow-Through Inhalation Exposure to Nanoparticles: Assessing Dosimetry and Intracellular Uptake of CeO(2) Nanoparticles*. Nanomaterials (basel) 10 (12).
Leibrock, L., Wagener, S., Singh, A.V., Laux, P., Luch, A., 2019. *Nanoparticle induced barrier function assessment at liquid-liquid and air-liquid interface in novel human lung epithelia cell lines*. Toxicol Res (camb) 8 (6), 1016–1027.
Singh, A.V., Romeo, A., Scott, K., Wagener, S., Leibrock, L., Laux, P., Luch, A., Kerkar, P., Balakrishnan, S., Dakua, S.P., Park, B.W., 2021. *Emerging Technologies for In Vitro Inhalation Toxicology*. Adv Healthc Mater 10 (18), e2100633.
Castranova, V., Porter, D., Millecchia, L., Ma, J.Y., Hubbs, A.F., Teass, A., 2002. *Effect of inhaled crystalline silica in a rat model: time course of pulmonary reactions*. Mol Cell Biochem 234–235 (1–2), 177–184.
Inoue, H., Shimada, A., Kaewamatawong, T., Naota, M., Morita, T., Ohta, Y., Inoue, K., Takano, H., 2009. *Ultrastructural changes of the air-blood barrier in mice after intratracheal instillation of lipopolysaccharide and ultrafine carbon black particles*. Exp Toxicol Pathol 61 (1), 51–58.
Nemmar, A., Hoet, P.H., Vanquickenborne, B., Dinsdale, D., Thomeer, M., Hoylaerts, M. F., Vanbilloen, H., Mortelmans, L., Nemery, B., 2002. *Passage of inhaled particles into the blood circulation in humans*. Circulation 105 (4), 411–414.
Manolova, V., Flace, A., Bauer, M., Schwarz, K., Saudan, P., Bachmann, M.F., 2008. *Nanoparticles target distinct dendritic cell populations according to their size*. Eur J Immunol 38 (5), 1404–1413.
Blank, F., Stumbles, P.A., Seydoux, E., Holt, P.G., Fink, A., Rothen-Rutishauser, B., Strickland, D.H., von Garnier, C., 2013. *Size-dependent uptake of particles by pulmonary antigen-presenting cell populations and trafficking to regional lymph nodes*. Am J Respir Cell Mol Biol 49 (1), 67–77.
Hammad, H., Lambrecht, B.N., 2007. *Lung dendritic cell migration*. Adv Immunol 93, 265–278.
Feray, A., Guillet, E., Szely, N., Hullo, M., Legrand, F.X., Brun, E., Rabilloud, T., Pallardy, M., Biola-Vidamment, A., 2021. *Synthetic Amorphous Silica Nanoparticles Promote Human Dendritic Cell Maturation and CD4+ T-Lymphocyte Activation*. Toxicol Sci 185 (1), 105–116.
Hamilton Jr., R.F., Thakur, S.A., Mayfair, J.K., Holian, A., 2006. *MARCO mediates silica uptake and toxicity in alveolar macrophages from C57BL/6 mice*. J Biol Chem 281 (45), 34218–34226.
Gallud, A., Bondarenko, O., Feliu, N., Kupferschmidt, N., Atluri, R., Garcia-Bennett, A., Fadeel, B., 2017. *Macrophage activation status determines the internalization of mesoporous silica particles of different sizes: Exploring the role of different pattern recognition receptors*. Biomaterials 121, 28–40.
Huaux, F., 2018. *Innate immunity to inhaled particles: A new paradigm of collective recognition*. Current Opinion in Toxicology 10, 7.
Adamson, I.Y., Prieditis, H., 1998. *Silica deposition in the lung during epithelial injury potentiates fibrosis and increases particle translocation to lymph nodes*. Exp Lung Res 24 (3), 293–306.
Wei, Q., Zhan, L., Juanjuan, B., Jing, W., Jianjun, W., Taoli, S., Yi'an, G., Wangsuo, W., 2012. *Biodistribution of co-exposure to multi-walled carbon nanotubes and nanodiamonds in mice*. Nanoscale Res Lett 7 (1), 473.
Mitchell, L.A., Gao, J., Wal, R.V., Gigliotti, A., Burchiel, S.W., McDonald, J.D., 2007. *Pulmonary and systemic immune response to inhaled multiwalled carbon nanotubes*. Toxicol Sci 100 (1), 203–214.
Chandrasekar, V., Jayanthi Panicker, A., Dey, A.K., Mohammad, S., Chakraborty, A., Kumar Samal, S., Dash, A., Bhadra, J., Suar, M., Khare, M., Prasad Dakua, S., Vikram Singh, A., 2024. *Integrated approaches for immunotoxicity risk assessment: challenges and future directions*. Discover. Toxicology 1 (9).
Ural, B.B., Caron, D.P., Dogra, P., Wells, S.B., Szabo, P.A., Granot, T., Senda, T., Poon, M. M.L., Lam, N., Thapa, P., Lee, Y.S., Kubota, M., Matsumoto, R., Farber, D.L., 2022. *Inhaled particulate accumulation with age impairs immune function and architecture in human lung lymph nodes*. Nat Med 28 (12), 2622–2632.

Zhang, J., Chen, Z., Shan, D., Wu, Y., Zhao, Y., Li, C., Shu, Y., Linghu, X., Wang, B., 2024. *Adverse effects of exposure to fine particles and ultrafine particles in the environment on different organs of organisms*. J Environ Sci (china) 135, 449–473.

Absher, M.P., Hemenway, D.R., Leslie, K.O., Trombley, L., Vacek, P., 1992. *Intrathoracic distribution and transport of aerosolized silica in the rat*. Exp Lung Res 18 (5), 743–757.

Kobayashi, T., Tsubokura, Y., Oshima, Y., Sasaki, T., Kawaguchi, K., Koga, K., Uchida, K., Shinohara, N., Ajimi, S., Kayashima, T., Nakai, M., Imatanaka, N., 2023. *Time-course analysis of pulmonary inflammation induced by intratracheal instillation of nanosized crystalline silica particles in F344 rats*. J Appl Toxicol 43 (5), 649–661.

Sasai, F., Rogers, K.L., Orlicky, D.J., Stem, A., Schaeffer, J., Garcia, G., Fox, J., Ray, M.S., Butler-Dawson, J., Gonzalez-Quiroz, M., Leiva, R., Taduri, G., Anutrakululchai, S., Venugopal, V., Madero, M., Glaser, J., Wijkstrom, J., Wernerson, A., Brown, J.M., Johnson, R.J., Roncal-Jimenez, C.A., 2022. *Inhaled silica nanoparticles cause chronic kidney disease in rats*. Am J Physiol Renal Physiol 323 (1), F48–F58.

Wang, H., Cui, J., Hao, X., Guo, L., Zhao, J., Wang, R., Liu, H., 2021. *Silicon, an important exposure marker in vivo in silicosis research*. Int Arch Occup Environ Health 94 (7), 1513–1522.

Hussein, A.M., Attia, D.I., Zayed, B.E.M., Rashed, L.A., El-Sherif, G.H.E., 2023. *Pulmonary Functions and Oxidative Stress Biomarkers Among Silica-Exposed Foundry Workers*. J Occup Environ Med 65 (5), 437–442.

Fenwick, S., Main, J., 2000. *Increased prevalence of renal disease in silica-exposed workers*. Lancet 356 (9233), 913–914.

ATSDR Toxicological profile for Silica. U.S. Department of Health and Human Services 2019.

Movia, D., Bruni-Favier, S., Prina-Mello, A., 2020. *In vitro Alternatives to Acute Inhalation Toxicity Studies in Animal Models-A Perspective*. Front Bioeng Biotechnol 8, 549.

Asgharian, B., Price, O.T., Oldham, M., Chen, L.C., Saunders, E.L., Gordon, T., Mikheev, V.B., Minard, K.R., Teeguarden, J.G., 2014. *Computational modeling of nanoscale and microscale particle deposition, retention and dosimetry in the mouse respiratory tract*. Inhal Toxicol 26 (14), 829–842.

Kolanjiyil, A.V., Kleinstreuer, C., Kleinstreuer, N.C., Pham, W., Sadikot, R.T., 2019. *Mice-to-men comparison of inhaled drug-aerosol deposition and clearance*. Respir Physiol Neurobiol 260, 82–94.

Gakis, G.P., Krikas, A., Neofytou, P., Tran, L., Charitidis, C., 2022. *Modelling the biodistribution of inhaled gold nanoparticles in rats with interspecies extrapolation to humans*. Toxicol Appl Pharmacol 457, 116322.

Han, D., Chen, R., Kan, H., Xu, Y., 2023. *The bio-distribution, clearance pathways, and toxicity mechanisms of ambient ultrafine particles*. Eco Environ Health 2 (3), 95–106.

De Vooght, V., Vanoirbeek, J.A., Haenen, S., Verbeken, E., Nemery, B., Hoet, P.H., 2009. *Oropharyngeal aspiration: an alternative route for challenging in a mouse model of chemical-induced asthma*. Toxicology 259 (1–2), 84–89.

Kunda, N.K., Price, D.N., Muttil, P., 2018. *Respiratory Tract Deposition and Distribution Pattern of Microparticles in Mice Using Different Pulmonary Delivery Techniques*. Vaccines (basel) 6 (3).

Yisrael, K., Drover, R.W., Shapiro, M.L., Anguiano, M., Kachour, N., Li, Q., Tran, E., Cocker 3rd, D.R., Lo, D.D., 2023. *Route of administration significantly affects particle deposition and cellular recruitment*. PLoS One 18 (11), e0289373.

Lazaridis, M., 2023. *Modelling approaches to particle deposition and clearance in the human respiratory tract*. Air Qual Atmos Health 16, 1989–2002.

Lakatos, H.F., Burgess, H.A., Thatcher, T.H., Redonnet, M.R., Hernady, E., Williams, J.P., Sime, P.J., 2006. *Oropharyngeal aspiration of a silica suspension produces a superior model of silicosis in the mouse when compared to intratracheal instillation*. Exp Lung Res 32 (5), 181–199.

Pauluhn, J., 2005. *Overview of inhalation exposure techniques: strengths and weaknesses*. Exp Toxicol Pathol 57 (Suppl 1), 111–128.

Song, Y., Zhao, L., Qi, Z., Zhang, Y., Cao, G., Li, R., Zhu, L., Yang, Z., Dong, C., Cai, Z., 2021. *Application of a real-ambient fine particulate matter exposure system on different animal models*. J Environ Sci (china) 105, 64–70.

Durand-Moreau, Q., 2023. *Urinary Silica Levels Might Reflect External Contamination of Exposed Workers*. J Occup Environ Med 65 (12), e813.

Dankovic, D.A., Naumann, B.D., Maier, A., Dourson, M.L., Levy, L.S., 2015. *The Scientific Basis of Uncertainty Factors Used in Setting Occupational Exposure Limits*. J Occup Environ Hyg 12 Suppl 1(sup1), S55–S68.

Calutu, I.M., Smarandescu, R.A., Rascu, A., 2022. *Biomonitoring Exposure and Early Diagnosis in Silicosis: A Comprehensive Review of the Current Literature*. Biomedicines 11 (1).